Journal of Structural Biology 186 (2014) 19–27

Contents lists available at ScienceDirect

Journal of Structural Biology

journal homepage: www.elsevier.com/locate/yjsbi

Key structural arrangements at the C-terminus domain of CETP suggest a potential mechanism for lipid-transfer activity

Victor García-González [a], Nadia Gutiérrez-Quintanar [a], Paola Mendoza-Espinosa [a], Pilar Brocos [b], Ángel Piñeiro [b], Jaime Mas-Oliva [a,c,*]

[a] Instituto de Fisiología Celular, Universidad Nacional Autónoma de México, 04510 México, D.F., Mexico
[b] Departamento de Física Aplicada, Facultad de Física, Universidad de Santiago de Compostela, Spain
[c] División de Investigación, Facultad de Medicina, Universidad Nacional Autónoma de México, Mexico

ARTICLE INFO

Article history:
Received 23 December 2013
Received in revised form 4 February 2014
Accepted 10 February 2014
Available online 14 February 2014

Keywords:
CETP
C-terminus domain
Lipid ordering
Secondary structure transitions
Lipid micelles

ABSTRACT

The cholesteryl-ester transfer protein (CETP) promotes cholesteryl-ester and triglyceride transfer between lipoproteins. We evaluated the secondary structure stability of a series of small peptides derived from the C-terminus of CETP in a wide range of pH's and lipid mixtures, and studied their capability to carry out disorder-to-order secondary structure transitions dependent of lipids. We report that while a mixture of phosphatidylcholine/cholesteryl-esters forms large aggregated particles, the inclusion of a series of CETP carboxy-terminal peptides in a stable α-helix conformation, allows the formation of small homogeneous micelle-like structures. This phenomenon of lipid ordering was directly connected to secondary structural transitions at the C-terminus domain when lysophosphatidic acid and lysophosphatidylcholine lipids were employed. Circular dichroism, cosedimentation experiments, electron microscopy, as well as molecular dynamics simulations confirm this phenomenon. When purified CETP is studied, the same type of phenomenon occurs by promoting the reorganization of lipid from large to smaller particles. Our findings extend the emerging view for a novel mechanism of lipid transfer carried out by CETP, assigning its C-terminus domain the property to accomplish lipid ordering through secondary structure disorder-to-order transitions.

1. Introduction

Several studies focused on the thermodynamic and kinetic analysis of lipid transfer between unilamellar phospholipid vesicles, show that this process is carried out through diffusion of monomers across a water interface. Here, velocity of exchange has been suggested to occur in function of a kinetic model of micellization that allows a semiquantitative prediction of the relative velocity of transfer (Aniansson et al., 1976). When the change in free energy values during lipid desorption from a phospholipid monolayer towards the water interface reach the highest point, the critical transition state corresponds to the last carbon atom to desorb from the monolayer, usually related to a high-energy consumption (Nichols, 1985). Therefore, the kinetic and thermodynamic parameters associated to this phenomenon allow the estimation of transfer efficiency for different lipid molecules (Fig. 1). For instance, cholesterol presents a significant energy barrier opposed to its desorption from a monolayer with a half-life of transference between two vesicles in the order of two hours, where ΔG_t corresponds to 55 kJ/mol. When the polarity of cholesterol is changed with the addition of a fatty acid, cholesteryl-oleate for example, transfer exceeds the scale of time for most biological processes since the operation would take 10^7 h to occur with a ΔG_t close to 94 kJ/mol. In contrast, the simple addition of a hydroxyl group promotes desorption relatively quickly, as it occurs in the case of 25-hydroxycholesterol, within a transfer time of around 2 min and a ΔG_t of 44 kJ/mol (Mc Lean and Phillips, 1984). From this type of analysis, we can conclude that transfer of neutral lipids through an aqueous phase is a costly biophysical event. Therefore, nature has developed a series of lipid transfer proteins such as CETP with unique structural properties designed to efficiently lower the energy barrier for transfer of cholesteryl-esters through an aqueous environment, not only between lipoproteins but also between the plasma membrane of cells and lipoproteins. Nevertheless, the critical physicochemical characteristics of the process associated to the key structural features of this protein that would explain the extremely efficient lipid transfer process, are still lacking. The

* Corresponding author at: Instituto de Fisiología Celular, Universidad Nacional Autónoma de México, 04510 México, D.F., Mexico. Fax: +52 5556225611.
E-mail address: jmas@ifc.unam.mx (J. Mas-Oliva).

http://dx.doi.org/10.1016/j.jsb.2014.02.002
1047-8477/

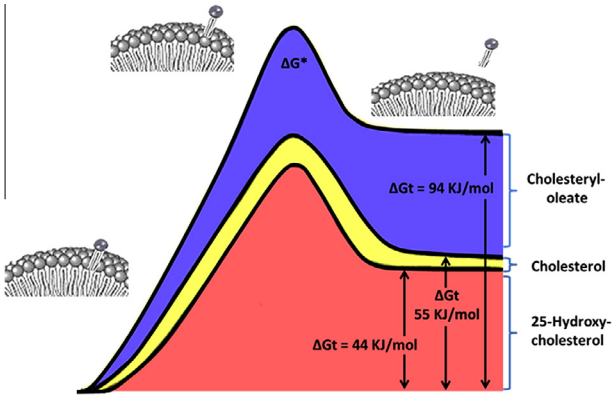

Fig.1. Free energy diagram for lipid exchange through an aqueous phase. The transfer of lipid molecules from unilamellar phospholipid vesicles to an aqueous phase proceeds through a *transition–state complex*, where an amphipathic lipid molecule is attached to the vesicle through its hydrophobic chain end. The formation of this activated-state complex is associated with a high energy of activation (ΔG^*), which exceeds the energy of transfer (ΔG_t) by an amount which is determined, in part, by the constraints of the lipid molecule with respect to the surface of the vesicle (modified from Mc Lean and Phillips, 1984).

present study proposes a new perspective for this process, taking into account that lipid transfer carried out by CETP associated to a minimum entropy change would maintain the thermodynamic equilibrium of the process.

Recently, the crystallographic structure of CETP at 2.2 Å resolution has revealed a 60 Å long tunnel filled with two cholesteryl-ester molecules (Qiu et al., 2007). Site specific mutagenesis has shown that a rather flexible carboxy-terminal region of CETP structured as an amphipathic α-helix, corresponds to a key region associated with the transfer process (Wang et al., 1995, 1993). Interestingly, since the boomerang-type concave surface of CETP corresponds to the radius curvature of high density lipoproteins (HDL), the position for the carboxy-terminal α-helix allows its optimal interaction with the surface of this type of lipoproteins through what we consider a corkscrew mechanism (Xicohtencatl-Cortes et al., 2004a,b). Most probably, the adopted orientation of this helical region is carried out parallel to the surface of HDL particles at the hydrophilic/hydrophobic interface of phospholipids as proposed by us for similar amphipathic helices contained in several human apolipoproteins (Bolaños-García et al., 1997; Xicohtencatl-Cortes et al., 2004a,b). Since neutral lipids have been suggested to be contained in CETP and the basic principles that allow neutral lipids to reach the core-tunnel have not been solved yet, based on our results we propose a lipid ordering mechanism that allows the formation of micelle-like structures supported by secondary structural transitions at the amphipathic carboxy-terminal region of CETP. This mechanism would allow the movement of lipid through an aqueous interface within accessible thermodynamic parameters.

2. Material and methods

L-α-Phosphatidylcholine (PC), 1-lauroyl-2-hydroxy-sn-glycero-3-phosphocholine (lyso-C_{12}PC), 1-hexanoyl-2-hydroxy-sn-glycero-3-phosphocholine (lyso-C_6PC) and 1-oleoyl-2-hydroxy-sn-glycero-3-phosphate (LPA) were obtained from Avanti Polar Lipids (Alabaster, AL). Cholesterol and cholesteryl-esters were purchased from Sigma–Aldrich (St. Louis, MO). Salts and buffers were purchased from J.T. Baker (Center Valley, PA).

2.1. Peptide synthesis

Peptides with a purity degree greater than 98% were synthesized by GenScript (Piscataway, NJ) and their identity and purity confirmed by mass spectrometry and HPLC analysis. Lyophilized peptides were dissolved in ammonium carbonate buffer (pH 9.5) to a concentration of 1.0 mg/mL. From this solution a further 1:5 dilution was carried out. To evaluate their secondary structure at pH 3.8 and 4.8, a sodium acetate buffer was used; for pH 6.3 and 7.2, a sodium phosphate buffer was used, and for pH's between 8.6 and 9.5, an ammonium carbonate buffer was employed. In all cases, ultrapure MilliQ water was always used together with a filtration step through 0.22 μm membrane filters. Peptide concentration was determined by measuring the peptide bond absorbance at 205 nm.

Peptide samples at a concentration of 200 μg/mL were incubated with the different lipid preparations for 12 h at 25 °C before their structural characterization employing circular dichroism, dynamic light scattering and electron microscopy. In the same manner, purified CETP was incubated with the different lipid preparations tested.

Several secondary structure predictors and servers were employed: the PSIPRED protein structure prediction server; Agadir an algorithm to predict the helical content of peptides; SOPMA (self-optimized prediction method with alignment); Protean DNA-Star program and Rosetta Design. Helical wheel representations were obtained using the Protean DNAStar program (Lasergene).

2.2. Circular dichroism (CD) spectroscopy

CD spectra were registered with an AVIV62DS spectropolarimeter (AVIV Instruments) at 25 °C employing far UV wavelengths (190–260 nm). Experiments were performed at a peptide concentration of 200 μg/mL in a 1 quartz path length cuvette running AVIV software. Spectra were recorded with a 1 mm bandwidth using 0.5 nm increments and 2.5 s accumulation time averaged over 3 scans. CD results are reported as mean molar ellipticity (Θ, deg cm^2 $dmol^{-1}$) considering the baseline correction.

2.3. Preparation of lipid mixtures

In order to obtain the desired concentrations of PC and cholesteryl-esters in the different mixtures prepared, lipids were mixed in chloroform and dried for 6 h under a gentle stream of N_2, and an additional period of 24 h in vacuum on a SpeedVac concentrator (Savant). Lipid mixtures were prepared with a molar ratio of PC 2 mM and cholesteryl-ester 100 μM. After drying, the lipids were resuspended in a phosphate buffer (NaH_2PO_4 33.3 mM, Na_2HPO_4 16.6 mM) at pH 6.8, and subsequently sonicated 15 s on/30 s off pulses for 4 cycles of 10 min in an ice bath under a flow of N_2 using a Sonifier 250 ultrasonicator (Branson). Samples were left to equilibrate for 2 h at 25 °C and centrifuged at 13,000 rpm for 10 min before being used.

2.4. Preparation of lyso-C_{12}PC micelles

The required amounts of lyso-C_{12}PC dissolved in chloroform were placed under a gentle stream of N_2 for 6 h, and an additional period of 22 h in vacuum. Samples were resuspended in a phosphate buffer (NaH_2PO_4 33.3 mM, Na_2HPO_4 16.6 mM) at pH 6.8 and 37 °C at a final concentration of 25 mM concentration. After this procedure, samples were kept 2 h at 25 °C, subsequently centrifuged at 13,000 rpm for 10 min at 12 °C and left to equilibrate for 2 h before being used.

2.5. Preparation of lysophosphatidic acid (LPA) micelles

The required amounts of LPA dissolved in chloroform were placed under a gentle flow of N_2 for 6 h, and an additional period of 12 h in vacuum. Samples were hydrated in a phosphate buffer (NaH_2PO_4 33.3 mM, Na_2HPO_4 16.6 mM) at a final concentration of 12.5 mM and further processed through 4 cycles of freezing in liquid N_2 and thawing at 37 °C. Solutions were kept 2 h at 25 °C and centrifuged for 10 min at 13,000 rpm.

2.6. Purification of CETP from human plasma

CETP was purified using a combination of ultra-centrifugation and several sequential chromatography steps (Ruiz-Noriega et al., 1994). Briefly, lipoprotein free plasma was isolated from freshly drawn human plasma by ultracentrifugation using a TLA 100.4 rotor. The lipoprotein clear fraction was loaded to a phenyl-Sepharose column pre-equilibrated with 4 M NaCl/10 mM Tris/2 mM EDTA pH 7.4. Proteins were eluted in two steps with 150 mM NaCl/10 mM Tris/2 mM EDTA and ultrapure MilliQ water. Fraction eluted with water was applied to an anion exchange column (Q Sepharose Fast Flow resin) and eluted with a 0–1.0 M NaCl gradient. Finally, the fraction obtained between 720 and 850 mM NaCl was applied to a concanavalin A-Sepharose column where specific CETP elution was achieved using α-methyl-D-mannoside (150 mM).

2.7. Dynamic light scattering (DLS)

DLS sample analysis was performed employing a Malvern Zetasizer Nano System at 25 °C immediately after CD measurements took place. The intensity of dispersed light was measured at an angle of 173°.

2.8. Molecular dynamics simulations

Coarse Grained (CG) simulations were performed with periodic boundary conditions using GROMACS MD engine version 3.3.3 (Van Der Spoel et al., 2005), and carried out in the NPT ensemble. Water and surfactant molecules were separately coupled to a Berendsen thermostat at 300 K with a common period of 1 ps. The pressure was isotropically controlled at 1 bar using a Berendsen barostat (Berendsen et al., 1984) with an isothermal compressibility of 5×10^{-5} bar^{-1}. The initial coordinates for CETP helix-X^{12} were obtained from available X-ray diffraction data (PDB: 2obd) (Qiu et al., 2007). The MARTINI force field (version 2.0) was employed to model all CG molecules (Marrink et al., 2007). As previously proposed by us for coarse grain structures, lipids were parameterized using four beads for the PC head and the first 2–3 CH_2 groups of the surfactant, and one up to three additional hydrophobic beads for the rest of the surfactant tail (Brocos et al., 2012). Random mixtures consisting of 234 CG lipid molecules, 23,415 Martini waters (equivalent to 93,660 atomistic water molecules), 1 CETP helix X^{12}, and 2Na^+ ions were introduced in rhombic dodecahedron boxes (edge length 15 nm). Each system was energy minimized using the steepest descent method and then three independent 5 μs long trajectories per each system performed starting from different initial random velocities. A 1.2 nm cut off was employed for non-bonded interactions. The L–J potential was smoothly shifted to zero between 0.9 and 1.2 nm. A similar approach was employed for electrostatic interactions, considering a Coulombic potential with a relative permittivity of 15 together with a shift function from 0 to 1.2 nm. The neighbor list was updated every 10 steps. The trajectory analysis was performed using tools of the GROMACS package, RasMol 2.7 and Pymol 0.99. More details can be found in a recent study from our group where CG simulations of micelles were performed using identical methods (Brocos et al., 2012).

2.9. Transmission electron microscopy

Peptides and CETP samples incubated with the different lipid mixtures tested were processed using a negative staining technique and visualized using transmission electron microscopy (NS-TEM). Samples (10 μL) were placed on carbon-coated copper grids (400 mesh) for 10 min at 25 °C before observations were made. Since in our experience contrast of negative stained samples can be improved by using copper-grids with slightly thicker carbon coatings, according to the color reference chart provided by the company Drukker International, we exposed copper grids to be used for the visualization of the lipid/CETP structures, to carbon vapor for longer periods of time until approximately a thickness of 100 nm was reached. Excess liquid was removed with Whatman paper and grids negatively stained for 5 min with uranyl acetate solution (2% w/v). Samples were dried for 20 min and NS-TEM images were acquired using a JEM-1200EX11 JEOL microscope at 70 kV with a 60,000× magnification.

2.10. Lipid/peptide cosedimentation assays and peptide bond spectroscopy

With the objective to evaluate binding of CETP derived peptides to lipid aggregates, cosedimentation experiments were performed using ultracentrifugation with an Optima TLX ultracentrifuge and a TLA-100.2 rotor (Palmer et al., 2009). Samples consisting of peptide, lipid, or peptide/lipid mixtures were centrifuged at 200,000*g* for 12 h to discard possible liposomal structures. When lyso-C_{12}PC and LPA were used, a further centrifugation step was carried out at 300,000*g* for 36 h, and 54 h respectively. In all cases 13 °C was maintained throughout the experiments. Supernatants were recovered and the remaining pellets resuspended in a phosphate buffer pH 7.2. Afterwards, absorbance of the supernatants and the remaining resuspended pellets was measured following the absorbance of peptide bonds at 205 and 218 nm.

2.11. Polyacrylamide gradient gel electrophoresis

Pellets obtained from the peptide/lipid cosedimentation assays were analyzed on non-denaturing gradient polyacrylamide gel electrophoresis. Samples were processed using 3–35%, 3–38% and 3–40% polyacrylamide gradients gels using a Tris–borate buffer during 16 h at 80 V. Gradient gels were stained with Coomassie blue G-250 (Toledo-Ibelles et al., 2010).

3. Results

The tridimensional view of the C-terminus region of CETP (aa 453–476) composed of a β-sheet (aa 453–462) and the native amphipathic α-helix (aa 465–476) named helix-X^{12} are shown in Fig. 2. When glutamic acid 465 is substituted by a cysteine residue, as it will be shown below, particular secondary structure characteristics are developed with this new model peptide known as helix-Y^{12} (Fig. 2A). Peptide helix-Y^{12} when placed in solution and incubated at different pH's, maintains most of its α-helical structure within a wide range of pH values (6.3–9.5) when studied by circular dichroism (CD) (Fig. 2B). This situation does not occur when native peptide helix-X^{12} is tested, since CD experiments show that secondary structure is lost and the peptide keeps a random conformation independently of pH values (Fig. 2C). The particular characteristics shown by peptide helix-Y^{12} constitute a key feature in the development of several patents carried out by

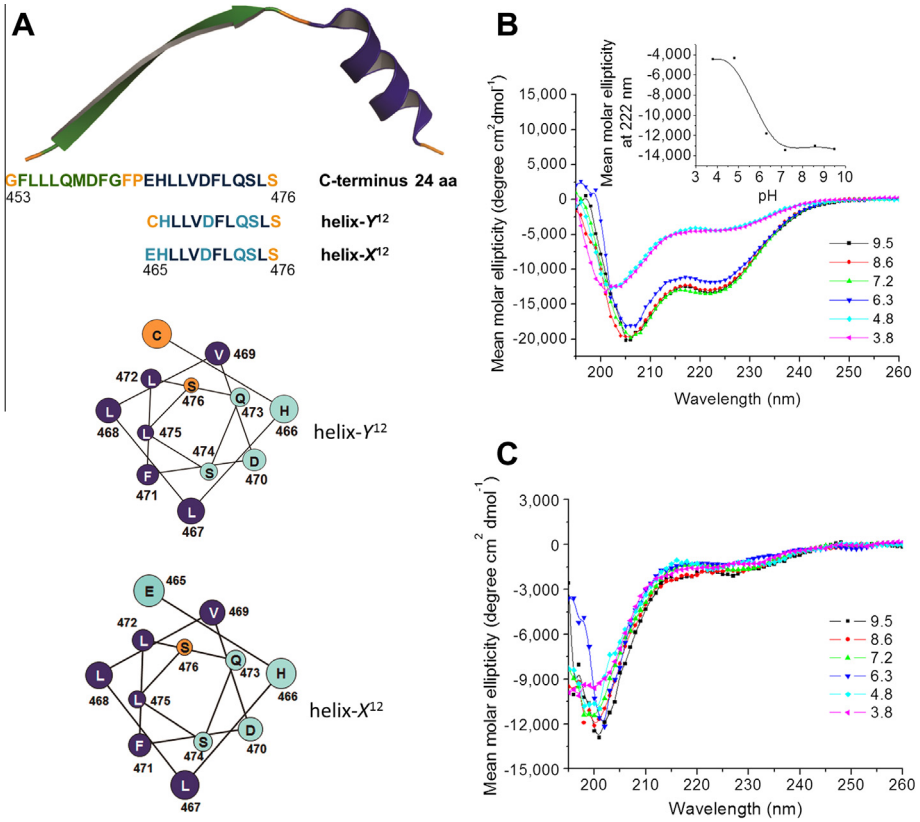

Fig.2. Structural characterization of peptides derived from the C-terminus of CETP. (A) Primary and secondary structures of the C-terminus region of CETP, showing helical wheel representations for peptide helix-X^{12} and for peptide helix-Y^{12} (PDB: 2obd); (B) employing CD, pH effect upon secondary structure of peptide helix-Y^{12} in the presence of phosphatidylcholine and cholesteryl-esters. Insert shows the change in mean molar ellipticity measured at 222 nm; (C) pH effect upon secondary structure of peptide helix-X^{12} in the presence of same lipids.

our group (Mas Oliva et al., 2012; Mas-Oliva and Alonso, 2010, 2007a; Mas Oliva and Alonso, 2007b).

On the other hand, under the same pH range, when a mixture of phosphatidylcholine and cholesteryl-esters are studied by dynamic light scattering (DLS), average aggregates of 30 nm are formed within a range that goes from 20 to 80 nm. This samples when studied by negative staining transmission electron microscopy (NS-TEM) confirmed the size of mostly large aggregates (Fig. 3A and B). It is interesting to observe that when peptide helix-Y^{12} is incubated together with the same lipid mixture at pH values close to 7.0, the formation of small homogeneous micelles with an average size of 6 nm is induced (Fig. 3C and D). As previously shown with CD experimentation, extreme pH values interfere with the formation of a well-defined peptide secondary structure and therefore the formation of only large aggregates is observed. This is consistent with previous results from our laboratory showing that electrostatic repulsions and a decrement of intramolecular hydrogen bonds induce the loss of secondary structure in peptides, and therefore aggregation is promoted as an initial step in the formation of amyloid like fibrils (Bolaños-García et al., 1998; García-González and Mas-Oliva, 2011). One of the factors that determine electrostatic repulsion is the net charge of peptides directly related to the pH value of the solution. In this sense, at neutral pH, the net charge of peptide helix-Y^{12} is −1.1, condition that optimally allows peptide interaction with lipid and therefore a complete micellization process takes place. In contrast, when pH 6.3 is tested, as shown in Fig. 3C part of the sample is maintained as large aggregates and part as small micelles. The explanation for this phenomenon is related to the fact that peptide helix-Y^{12} at pH 6.3 presents a net charge of −0.6, far from an optimal condition for peptide/lipid interaction. pH values close to the isoelectric points of both peptides helix-Y^{12} (5.09) and helix-X^{12} (4.17) tend to form large aggregates.

Our results show that peptide helix-Y^{12} when tested close to physiological pH values, allows the stabilization of the amphipathic carboxy-terminal α-helix and therefore the ability to promote the organization of micelle-like lipid structures. Under the same conditions, although in a smaller degree, peptide helix-X^{12} showing a random conformation in solution, in the presence of lipid aggregates is also able to perform the lipid ordering phenomenon (Fig. 3E and F).

When we employ specific lipids such as 12-lysophosphatidylcholine (lyso-C_{12}PC) and lysophosphatidic acid (LPA), known by us to promote the formation of α-helices with amphipathic peptides, peptide helix-X^{12} is able to keep a stable α-helical conformation (Figs. 4A and B; 5A and B) and when visualized by NS-TEM also able to promote a lipid ordering effect (Figs. 4C and D; 5C and D). Therefore, for this process to occur, we can conclude that the presence of a well-structured amphipathic α-helix seems to be one of the key factors to achieve the phenomenon described. In order to further characterize peptide/lipid interactions and the fact that peptides promote the micellization process, employing the same concentrations that range from 0 to 40 mM for lyso-C_{12}PC and 0–10 mM for LPA, peptide/lipid cosedimentation assays were performed. Spectroscopy of peptide bonds associated to pellets obtained after ultraspeed centrifugation showed that while peptide helix-X^{12} in solution does not sediment, the presence of lipid in solution allows the formation of micelles, and only at this condition peptide sedimentation takes place (Figs. 4E and 5E). When a lower centrifugation speed known to sediment liposome-like

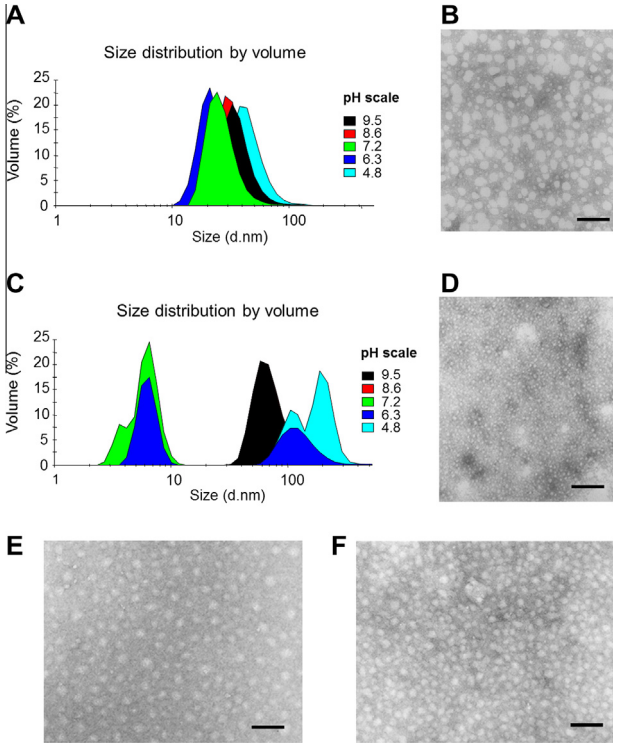

Fig.3. Formation of micelle-like structures. (A) Particle size distribution of samples composed exclusively of phosphatidylcholine and cholesteryl-esters measured by DLS using a pH range of 4.8–9.5; (B) same lipid sample at pH 7.2 studied by NS-TEM; (C) same lipid mixture plus the addition of peptide helix-Y^{12} studied by DLS. Particle size distribution at pH 8.6 not shown since it exactly corresponds to result obtained at pH 9.5; (D) representative image of mixture lipid/helix-Y^{12} at pH 7.2 obtained with NS-TEM employing the same experimental conditions; (E) electron microscopy image corresponding to the control mixture of phosphatidylcholine and cholesteryl-esters studied at pH 7.2, and (F) plus the addition of peptide helix-X^{12}. For every EM image, bar indicates 100 nm.

structures was employed during experimentation with both lipids, either in the absence or the presence of peptide helix-X^{12}, negligible absorbance values were found associated with the almost non-existent pellets, indicating that the formation of liposomes is not a major factor to consider under the experimental conditions carried out throughout our study (Fig. 4E). Furthermore, non-denaturing polyacrylamide gradient gel electrophoresis support the view that micelle formation, promoted by the presence of peptide helix-X^{12}, initiates at low lipid concentrations as shown by the presence of bands only when the optimal association between lipid and peptide is achieved (Figs. 4F and 5F).

From these experiments, it is interesting to point out that the micellization process takes place precisely at the point when peptide helix-X^{12} presents a structural transition from a disordered state to an α-helix when circular dichroism data is analyzed (Figs. 4A and B; 5A and B). Precisely at this point where secondary structure transitions and lipid ordaining take place, the molar relationship between lipids tested and helix-X^{12} corresponds to one order of magnitude difference with an average of 35 and 18 molecules of lyso-C_{12}PC and LPA, respectively, associated to one peptide. As shown in Fig. 5F, an increase in LPA concentration does not affect the amount of helix-X^{12}/lipid micelles trapped in the gels, indicating that due to the fixed number of peptides placed in solution, practically all peptide units are found associated to lipid micelles independently of the fact that lipid concentration is being increased. Under these conditions, the physicochemical properties shown by the peptide such as high hydrophobicity and high hydrophobic moment (μH) warranty a strong driving force towards micelle formation.

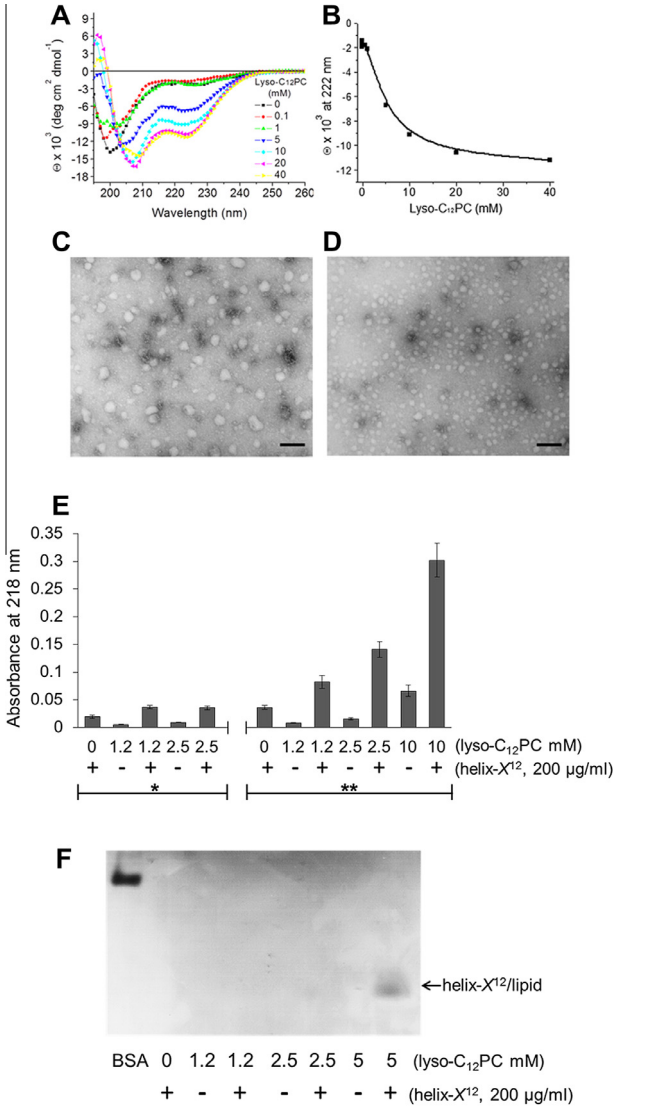

Fig.4. Lysophosphatidylcholine promotes a stable α-helix conformation of peptide helix-X^{12}. (A) Circular dichroism and secondary structure changes observed in peptide helix-X^{12} modulated by the presence of 12-lysophosphatidylcholine; (B) mean molar ellipticity values at 222 nm revealed an increase in the α-helix content of peptide helix-X^{12}; (C) lysophosphatidylcholine aggregates (10 mM) studied by NS-TEM at pH 7.2; (D) effect of the presence of peptide helix-X^{12} upon the same lipid mixture. For every EM image, bar indicates 100 nm; (E) lysophosphatidylcholine/peptide helix-X^{12} cosedimentation assay and peptide bond spectroscopy. Data shown are the mean ± SEM of 3 experiments. Cosedimentation assays performed at 200,000*g* for 12 h (*) and 300,000*g* for 36 h (**); (F) non denaturing polyacrylamide gradient gel electrophoresis of pellets obtained from lysophosphatidylcholine/peptide helix-X^{12} cosedimentation assays. The 3–38% gel was stained with Coomassie blue G-250.

Taking into account these considerations, molecular dynamics experimentation also allowed us to evaluate the behavior of peptide helix-X^{12} in a well controlled lipid environment consisting of a relationship of 234 lipid molecules, ~93,700 water molecules and one peptide helix-X^{12}. As shown in Fig. 6A, the interaction of peptide helix-X^{12} with 12-lysophosphatidylcholine aggregates promotes the formation of micellar-like structures with an average lower than 70 lipid molecules and one peptide per particle, showing diameters around 5 nm. It is interesting to observe that lipid particles that do not associate with a peptide molecule tend to associate between them, while peptide-associated micelles seem to be stable and stay in solution by themselves. The same lipid ordering phenomenon is observed when 16-lysophosphatidylcholine is

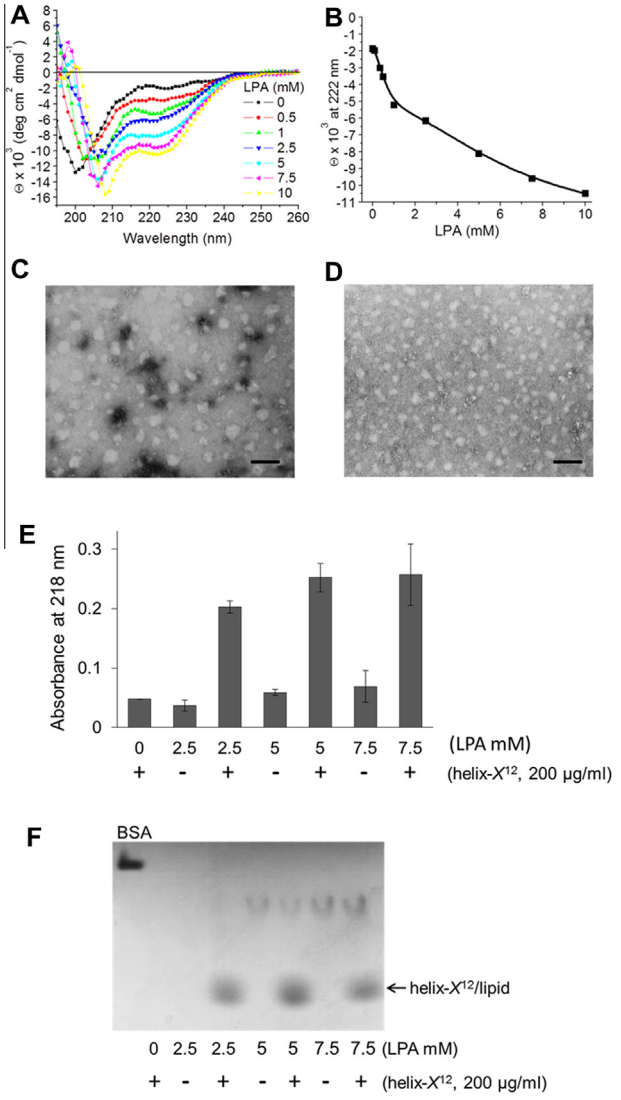

Fig.5. Lysophosphatidic acid promotes a stable α-helix conformation of peptide helix-X^{12}. (A) Circular dichroism and secondary structure changes of peptide helix-X^{12} modulated by the presence of LPA; (B) mean molar ellipticity values at 222 nm revealed an increase in α-helix content of peptide helix-X^{12} while increasing lipid concentration; (C) LPA (10 mM) aggregates studied by NS-TEM at pH 7.2; (D) effect of the presence of peptide helix-X^{12} on the same lipid mixture. For every EM image, bar indicates 100 nm; (E) LPA/peptide helix-X^{12} cosedimentation assay and peptide bond spectroscopy. Data shown are the mean ± SEM of 3 experiments. Cosedimentation assays performed at 300,000*g* for 54 h; (F) non denaturing polyacrylamide gradient gel electrophoresis of pellets obtained from LPA/peptide helix-X^{12} cosedimentation assays. The 3–40% gel was stained with Coomassie blue G-250.

employed (Fig. 6B). Lipids such as 6-lysophosphatidylcholine that presents a high cmc shows the tendency to effectively bind to peptide helix-X^{12} and organize peptide-associated micelles even before lipid molecules can form micelles by themselves (Fig. 6C). These results provide new evidence and further support the proposal that peptide helix-X^{12} located in CETP could facilitate the process of lipid ordering through the formation of micelle-like structures.

From this type of experiments and in order to prove that lipid ordering and the micellization concept might be also carried out by the complete protein, the need to perform a series of experiments employing native CETP became evident. As previously shown with peptides helix-Y^{12} and helix-X^{12} when incubated in a solution containing lipid aggregates, purified CETP isolated from human plasma (Fig. 7), shows the capability to induce a similar phenomenon of lipid ordering as shown above for peptides (Fig. 8). We believe, as previously demonstrated by us employing a series of amphipathic peptides derived from several apolipoproteins (Mendoza-Espinosa et al., 2008; Bolaños-García et al., 2001), reordering of lipids from large non-homogenous to smaller more homogeneous particles could be accomplished due to the ability of CETP, through its amphipathic C-terminus domain, to promote an equilibrium shift and optimize the possibility for binding lipids in an aqueous solution.

The results presented in this study employing purified lipids and the use of artificial lipid structures, places us in an optimal position to experiment and better understand now the role for the C-terminus sequence of CETP during lipid transfer amongst human lipoproteins. According to our working hypothesis, present experimentation is being carried out by our group employing isothermal compression of binary Langmuir–Blodgett monolayers (Xicohtencatl-Cortes et al., 2004a,b) and interferometric surface force measurements (Ramos et al., 2008) in order to be able to elucidate and understand, for instance, lipid transfer and the role of surface pressure on HDL particles and its association to local disorder in proteins such as CETP and Lecithin cholesterol acyltransferase (LCAT) (Aguilar-Espinosa et al., 2013).

4. Discussion

Since apparently lipoprotein stabilization is mostly based on a kinetic rather than a thermodynamic process, HDL particles for instance, can be considered unstable particles contained in a kinetic trap (Mehta et al., 2003). Due to this instability, several procedures that include thermal (Sparks et al., 1992) and chaotropic (Mehta et al., 2003) treatment, can easily release the particle from this trap. Our proposal presenting an alternative possibility that would explain the efficient lipid transfer activity carried out by CETP, could take advantage of this fact when the protein binds to an HDL particle releasing the lipoprotein from this kinetic trap (Guha et al., 2008). The release and further stabilization carried out at the surface of an HDL particle could be triggered by HDL lipids when binding around the amphipathic C-terminus domain of CETP. This new structural condition suggests that changes in the curvature present in CETP along its *X*-axis could be involved with the trigger mechanism that controls binding and release of CETP from the surface of a lipoprotein (Hall and Qiu, 2011; Mendoza-Espinosa et al., 2008), as well as to the phenomenon of HDL remodeling (Maugeais et al., 2013; Niesor et al., 2010).

Although recently Zhang et al. (2012) based on electron microscopy images have proposed that lipid transfer might be carried out through the formation of ternary complexes between two lipoprotein particles and CETP, their interpretation does not take into account the fact that the C-terminus amphipathic α-helix, proven to be essential for the transfer process, is not involved in their model. Moreover, molecular dynamics simulation studies have recently shown that CETP is not able to penetrate further than the phosphate groups of a phospholipid monolayer (Koivuniemi et al., 2012). Also, there is no mention as to how triglycerides and phospholipids together with cholesteryl-esters might be transferred. Although two cholesteryl-ester molecules have been tightly associated to the tertiary structure of CETP, the presence of neutral lipids in the core space of the protein could be directly associated to the maintenance of its structural stability. In this respect, it has been reported that the bactericidal/permeability-increasing protein (BPI) that shows a potent antimicrobial action and binds to lipopolysaccharides, presents a striking structural similarity with CETP. It is suggested that despite this close similarity, BPI presents a more open structure and a completely different C-terminus sequence in comparison to CETP, phenomenon must probably related

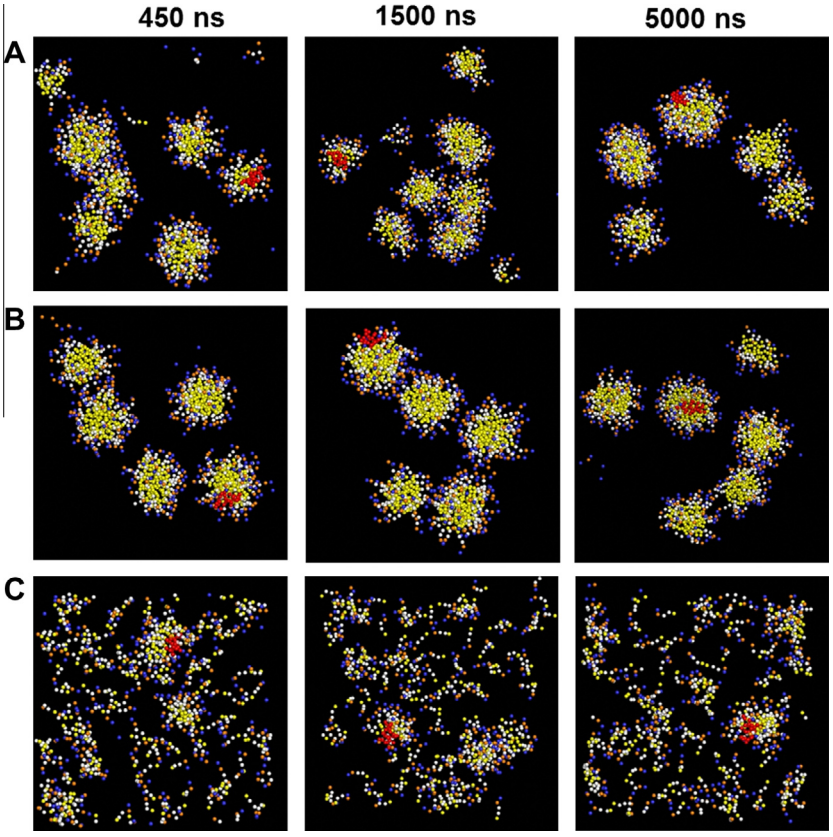

Fig.6. Molecular dynamics simulations of lipids in the presence of peptide helix-X^{12}. Snapshots were taken at 450, 1500 and 5000 ns. Peptide helix-X^{12} incubated with 12-lysophosphatidylcholine (A), and 16-lysophosphatidylcholine (B). (C) Under incubation with 6-lysophosphatidylcholine monomers, peptide helix-X^{12} promotes de organization of micelles around itself. Peptide molecules are represented in red and water molecules are not shown for clarity.

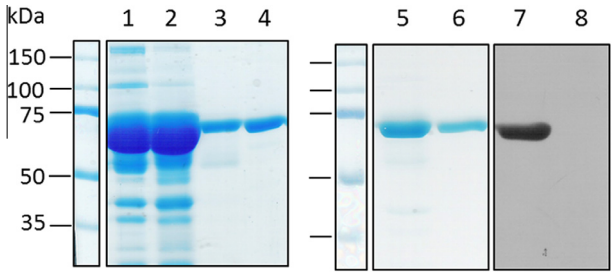

Fig.7. Purification of CETP from human plasma. (1) Lipoprotein free plasma, (2) hydrophobic interaction chromatography fraction obtained with water elution, (3) anionic-exchange chromatography fraction eluted with a 0–1 M sodium chloride gradient (720–850 mM), (4) bovine serum albumin (BSA), (5) purified CETP, (6) BSA. Lanes (7) and (8) show the Western-blot analysis of fractions 5 and 6, respectively, employing an anti-CETP monoclonal antibody.

to the fact that BPI apparently does not bind cholesteryl-esters (Beamer, 2003). If we take into account that the amphipathic C-terminus α-helix of CETP might be considered as an orienting force region in the same fashion as detergents do (Tanford, 1978), the proposal we describe in this study could support an efficient transference of lipid molecules within energetically suitable parameters.

The presence of conformational transitions associated to the thermodynamics of the process similar to the one described here for the C-terminus domain of CETP, has been documented for other lipid-binding proteins such as apolipoprotein A-1 (Kono et al., 2008; Oda et al., 2003) Since the C-terminus domain of CETP maintains a high intramolecular flexibility with a high factor-*B* associated to the interaction with lipids, this property must be directly associated to the type and concentration of specific lipids that would allow or prevent shifts in secondary structure (García-González and Mas-Oliva, 2013; Koivuniemi et al., 2012). For instance, it has been described that LPA at cmc, when placed in contact with β2-microglobulin, promotes the formation and extension of amyloid fibrils (Pál-Gábor et al., 2009; Ookoshi et al., 2008). However, we found that employing a wide range of concentrations above cmc, LPA and to a lesser extent lysophosphatidylcholine, promote a shift towards α-helical structures and prevent the formation of amyloid fibrils when peptide helix-*Z* ($D_{470}N$ mutation) derived of the C-terminus domain of CETP is studied (García-González and Mas-Oliva, 2013). Therefore, the control of conformational changes at specific sites of proteins given by specific lipids might be taken as the basis for the design of lipid-like molecules which could maintain or stabilize the native state of proteins prone for aggregation (García-González and Mas-Oliva, 2012).

In conclusion, the type of molecular organization described in our study carried out by the C-terminal segment of CETP following disorder-to-order secondary structure transitions controlled by the presence of specific lipids, in our view might be understood as an example of a molecular switch (García-González and Mas-Oliva, 2013; Mendoza-Espinosa et al., 2009). This would allow CETP to control function under specific metabolic conditions and keep its transfer activity associated to a minimum entropy change related to the formation of micelle-like structures at the C-terminal segment of the protein, process that would dramatically lower the energy barrier for lipid transfer to occur through aqueous media.

Acknowledgments

We thank Blanca Delgado for technical assistance, Rodolfo Paredes for technical support during NS-TEM experimentation

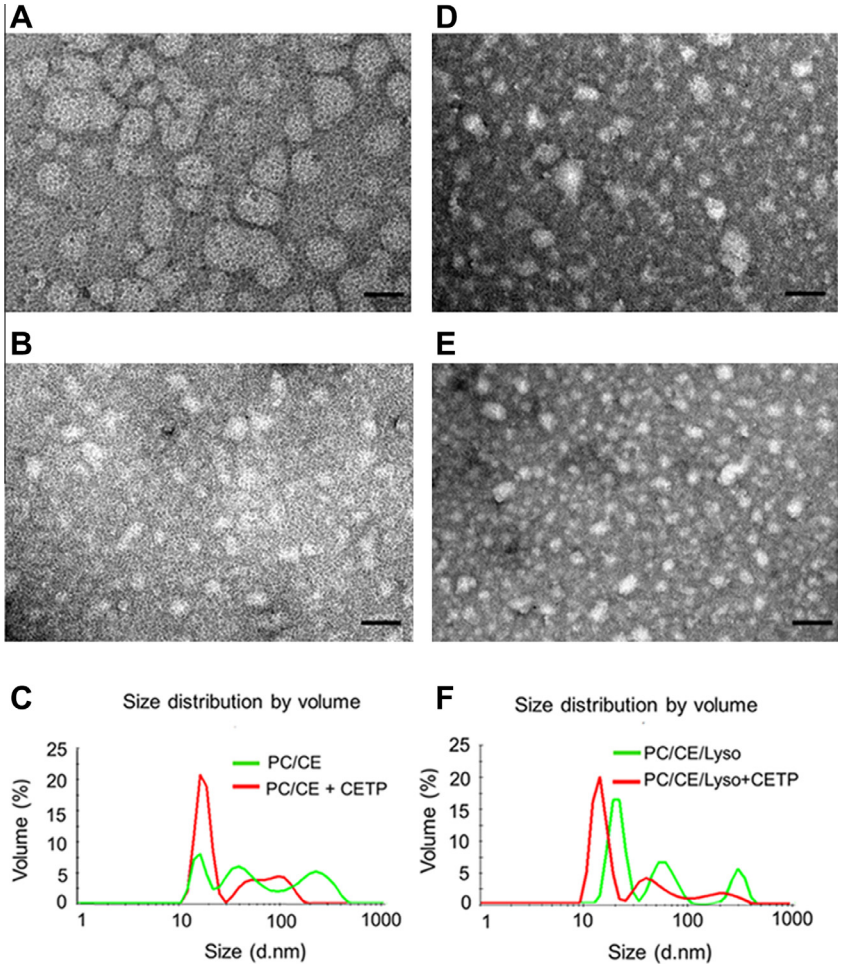

Fig.8. Lipid reorganization induced by CETP. (A) Lipid aggregates composed of phosphatidylcholine and cholesteryl-esters analyzed by NS-TEM; (B) incubation of the same lipid sample plus the addition of CETP generates better organized lipid particles; (C) particle size distribution of both samples evaluated through DLS; (D) lipid aggregates composed of phosphatidylcholine, cholesteryl-esters (CE) and lysophosphatidylcholine (Lyso); (E) effect of CETP upon the same lipid mixture and (F) samples evaluated by DLS. Protein used at 0.11 μM and lipids at 12.7 μM. Bar indicates 100 nm.

and Paola Toledo-Ibelles for help with PAGE. This study was supported by Consejo Nacional de Ciencia y Tecnología, México (CONACyT grant 083673) and DGAPA/UNAM (grant IN205711), both awarded to J.M.-O., V.G.-G., N.G.-Q., P.M.-E. are recipients of a studentship from CONACyT.

References

Aguilar-Espinosa, S.L., Mendoza-Espinosa, P., Delgado-Coello, B.A., Mas-Oliva, J., 2013. Lecithin cholesterol acyltransferase (LCAT) activity in the presence of Apo-AI-derived peptides exposed to disorder-order conformational transitions. Biochem. Biophys. Res. Commun. http://dx.doi.org/10.1016/j.bbrc.2013.10.089.

Aniansson, E.A.G., Wall, S.N., Almgren, M., Hoffmann, H., Kielmann, I., et al., 1976. Theory of the kinetics of micellar equilibria and quantitative interpretation of chemical relaxation studies of micellar solutions of ionic surfactants. J. Phys. Chem. 80, 905–922.

Beamer, L.J., 2003. Structure of human BPI (bactericidal/permeability-increasing protein) and implications for related proteins. Biochem. Soc. Trans. 31, 791–794.

Berendsen, H.J.C., Postma, J.P.M., Van Gunsteren, W.F., Dinola, A., Haak, J.R., 1984. Molecular dynamics with coupling to an external bath. J. Chem. Phys. 81, 3684–3690.

Bolaños-García, V.M., Ramos, S., Castillo, R., Xicohtencatl-Cortes, J., Mas-Oliva, J., 2001. Monolayers of apolipoproteins at the air/water interfaces. J. Phys. Chem. B 105, 5757–5765.

Bolaños-García, V.M., Soriano-García, M., Mas-Oliva, J., 1998. Stability of the C-terminal peptide of CETP mediated through an (i, i+4) array. Biochim. Biophys. Acta 1384, 7–15.

Bolaños-García, V.M., Soriano-García, M., Mas-Oliva, J., 1997. CETP and exchangeable apoproteins: common features in lipid binding activity. Mol. Cell. Biochem. 175, 1–10.

Brocos, P., Mendoza-Espinosa, P., Castillo, R., Mas-Oliva, J., Piñeiro, Á., 2012. Multiscale molecular dynamics simulations of micelles: coarse-grain for self-assembly and atomic resolution for finer details. Soft Matter 8, 9005–9014.

García-González, V., Mas-Oliva, J., 2013. Amyloid fibril formation of peptides derived from the C-terminus of CETP modulated by lipids. Biochem. Biophys. Res. Commun. 434, 54–59.

García-González, V.G., Mas-Oliva, J., 2012. El Concepto de Enfermedad Asociado a la Conformación de Proteínas, first ed. Universidad Nacional Autónoma de México and El Manual Moderno, México.

García-González, V., Mas-Oliva, J., 2011. Amyloidogenic properties of a D/N mutated 12 amino acid fragment of the C-terminal domain of the cholesteryl-ester transfer protein (CETP). Int. J. Mol. Sci. 12, 2019–2035.

Guha, M., Gao, X., Jayaraman, S., Gursky, O., 2008. Correlation of structural stability with functional remodeling of high-density lipoproteins: the importance of being disordered. Biochemistry 47, 11393–11397.

Hall, J., Qiu, X., 2011. Structural and biophysical insight into cholesteryl ester-transfer protein. Biochem. Soc. Trans. 39, 1000–1005.

Koivuniemi, A., Vuorela, T., Kovanen, P.T., Vattulainen, I., Hyvönen, M.T., 2012. Lipid exchange mechanism of the cholesteryl ester transfer protein clarified by atomistic and coarse-grained simulations. PLoS Comput. Biol. 8, e1002299.

Kono, M., Okumura, Y., Tanaka, M., Nguyen, D., Dhanasekaran, P., et al., 2008. Conformational flexibility of the N-terminal domain of apolipoprotein a–I bound to spherical lipid particles. Biochemistry 47, 11340–11347.

Marrink, S.J., Risselada, H.J., Yefimov, S., Tieleman, D.P., De Vries, A.H., 2007. The MARTINI force field: coarse grained model for biomolecular simulations. J. Phys. Chem. B 111, 7812–7824.

Mas Oliva, J., García González, V., Delgado Coello, B.A., Pérez, A., 2012. Fabricación de una Vacuna Terapéutica de Aplicación Nasal contra el Desarrollo de la

Aterosclerosis y el Hígado Graso. MX patent application number MX/a/2012/007682.
Mas-Oliva, J., Alonso, A.L., 2010. System for the quantification of the cholesterol ester transfer protein in biological and synthetic samples. US patent 7,749,721.
Mas-Oliva, J., Alonso, A.L., 2007a. System for the quantification of the cholesterol ester transfer protein in biological and synthetic samples. EP patent 1,242,446.
Mas Oliva, J., Alonso, A.L., 2007b. Sistema para la Cuantificación de la Proteína Transferidora de Ésteres de Colesterol en Muestras Biológicas y Sintéticas. MX patent 246,945.
Maugeais, C., Perez, A., von der Mark, E., Magg, C., Pflieger, P., et al., 2013. Evidence for a role of CETP in HDL remodeling and cholesterol efflux: role of cysteine 13 of CETP. Biochim. Biophys. Acta 1831, 1644–1650.
Mc Lean, L.R., Phillips, M.C., 1984. Kinetics of phosphatidylcholine and lysophosphatidylcholine exchange between unilamellar vesicles. Biochemistry 23, 4624–4630.
Mehta, R., Gantz, D.L., Gursky, O., 2003. Human plasma high-density lipoproteins are stabilized by kinetic factors. J. Mol. Biol. 328, 183–192.
Mendoza-Espinosa, P., García-González, V., Moreno, A., Castillo, R., Mas-Oliva, J., 2009. Disorder-to-order conformational transitions in protein structure and its relationship to disease. Mol. Cell. Biochem. 330, 105–112.
Mendoza-Espinosa, P., Moreno, A., Castillo, R., Mas-Oliva, J., 2008. Lipid dependant disorder-to-order conformational transitions in apolipoprotein CI derived peptides. Biochem. Biophys. Res. Commun. 365, 8–15.
Nichols, J.W., 1985. Thermodynamics and kinetics of phospholipid monomer-vesicle interaction. Biochemistry 24, 6390–6398.
Niesor, E.J., Magg, C., Ogawa, N., Okamoto, H., von der Mark, E., et al., 2010. Modulating cholesteryl ester transfer protein activity maintains efficient pre-β-HDL formation and increases reverse cholesterol transport. J. Lipid Res. 51, 3443–3454.
Oda, M.N., Forte, T.M., Ryan, R.O., Voss, J.C., 2003. The C-terminal domain of apolipoprotein A–I contains a lipid-sensitive conformational trigger. Nat. Struct. Biol. 10, 455–460.
Ookoshi, T., Hasegawa, K., Ohhashi, Y., Kimura, H., Takahashi, N., et al., 2008. Lysophospholipids induce the nucleation and extension of beta2-microglobulin-related amyloid fibrils at a neutral pH. Nephrol. Dial. Transplant. 23, 3247–3255.
Pál-Gábor, H., Gombos, L., Micsonai, A., Kovács, E., Pretrik, É., et al., 2009. Mechanism of lysophosphatidic acid-induced amyloid fibril formation of beta (2)-microglobulin in vitro under physiological conditions. Biochemistry 48, 5689–5699.
Palmer, S.M., Playford, M.P., Craig, S.W., Schaller, M.D., Campbell, S.L., 2009. Lipid binding to the tail domain of vinculin: specificity and the role of the N and C termini. J. Biol. Chem. 284, 7223–7231.
Qiu, X., Mistry, A., Ammirati, M.J., Chrunyk, B.A., Clark, R.W., et al., 2007. Crystal structure of cholesteryl ester transfer protein reveals a long tunnel and four bound lipid molecules. Nat. Struct. Mol. Biol. 14, 106–113.
Ramos, S., Campos-Terán, J., Mas-Oliva, J., Nylander, T., Castillo, R., 2008. Forces between hydrophilic surfaces adsorbed with apolipoprotein AII alpha helices. Langmuir 24, 8568–8575.
Ruiz-Noriega, M., Silva-Cárdenas, I., Delgado-Coello, B., Zentella-Dehesa, A., Mas-Oliva, J., et al., 1994. Membrane bound CETP mediates the transfer of free cholesterol between lipoproteins and membranes. Biochem. Biophys. Res. Commun. 202, 1322–1328.
Sparks, D.L., Lund-Katz, S., Phillips, M.C., 1992. The charge and structural stability of apolipoprotein A–I in discoidal and spherical recombinant high density lipoprotein particles. J. Biol. Chem. 267, 25839–25847.
Tanford, C., 1978. The hydrophobic effect and the organization of living matter. Science 200, 1012–1018.
Toledo-Ibelles, P., García-Sánchez, C., Ávila-Vazzini, N., Carreón-Torres, E., Posadas-Romero, C., et al., 2010. Enzymatic assessment of cholesterol on electrophoresis gels for estimating HDL size distribution and plasma concentrations of HDL subclasses. J. Lipid Res. 51, 1610–1617.
Van Der Spoel, D. et al., 2005. GROMACS: fast, flexible, and free. J. Comput. Chem. 26, 1701–1718.
Wang, S., Kussie, P., Deng, L., Tall, A., 1995. Defective binding of neutral lipids by a carboxyl-terminal deletion mutant of cholesteryl ester transfer protein. Evidence for a carboxyl-terminal cholesteryl ester binding site essential for neutral lipid transfer activity. J. Biol. Chem. 270, 612–618.
Wang, S. et al., 1993. Point mutagenesis of carboxyl-terminal amino acids of cholesteryl ester transfer protein. Opposite faces of an amphipathic helix important for cholesteryl ester transfer or for binding neutralizing antibody. J. Biol. Chem. 268, 1955–1959.
Xicohtencatl-Cortes, J., Castillo, R., Mas-Oliva, J., 2004a. In search of new structural states of exchangeable apolipoproteins. Biochem. Biophys. Res. Commun. 324, 467–470.
Xicohtencatl-Cortes, J., Mas-Oliva, J., Castillo, R., 2004b. Phase transitions of phospholipid monolayers penetrated by apolipoproteins. J. Phys. Chem. B 108, 7307–7315.
Zhang, L., Yan, F., Zhang, S., Lei, D., Charles, M.A., et al., 2012. Structural basis of transfer between lipoproteins by cholesteryl ester transfer protein. Nat. Chem. Biol. 8, 342–349.